

1 **Integrated analysis of high-throughput sequencing-based lncRNA-mediated ceRNA network in**
2 **Hepatic Alveolar Echinococcosis**

3 Zhen Liu¹, Chang-zhen Shang³, Jin-peng Wang¹, Zhi-gang Gai¹, Fu-cai Ma², Pan Xia¹, Yan Wang²,
4 Xiao Yang², Hai-hong Zhu^{2*}

5 1: Department of Graduate School, Qinghai University, Xining, Qinghai Province, China

6 2: Department of General Surgery, Qinghai Provincial People's Hospital, Xining, Qinghai Province,
7 China

8 3: Department of Hepatobiliary Surgery, Sun Yet-Sen Memorial Hospital, Sun Yet-Sen University,
9 Shanwei, Guangdong Province, China

10 **Abstract:**

11 **Background:**

12 Numerous studies have indicated that long non-coding RNAs (lncRNAs) can modulate the expression of
13 target gene mRNAs by adsorbing microRNAs (miRNAs). The lncRNA-miRNA-mRNA ceRNA
14 network has been theorized to play an indispensable role in many types of tumors, and has been garnering
15 increasing attention. However, the role of the lncRNA-associated ceRNA regulatory network in Hepatic
16 Alveolar Echinococcosis (HAE) remains unclear and requires further exploration.

17 **Methods:**

18 In this study, high-throughput sequencing was performed on lesion tissues and adjacent tissues from
19 three patients with Hepatic Alveolar Echinococcosis (HAE) to identify differentially expressed
20 RNAs. We utilized Cytoscape (version 3.10.1) to construct the lncRNA-miRNA-mRNA ceRNA
21 network based on the interactions from the miRcode, miRTarBase, miRDB, and TargetScan databases,
22 and identified hub lncRNAs from within the ceRNA network. Through the use of the "clusterProfiler"
23 package in R, we performed Gene Ontology (GO) and Kyoto Encyclopedia of Genes and Genomes

*Corresponding author: Hai-Hong Zhu

Department of General Surgery, Qinghai Provincial People's Hospital, Xining, Qinghai Province,
China.

Email: zhuhaihong1214@126.com

24 (KEGG) pathway annotations for the DEGs (Differentially Expressed Genes) within the ceRNA network.
25 Concurrently, we utilized these DEGs to construct a protein-protein interaction network (PPI). Finally,
26 an analysis was conducted on the PCBP1-AS1-miR-20b-5p/CAPRIN2 axis within the ceRNA network.

27 **Results:**

28 In HAE, a total of 979 differentially expressed lncRNAs (DELncRNAs) and 870 differentially expressed
29 mRNAs (DEmRNAs) were identified. An HAE-specific ceRNA network comprising 11 lncRNAs, 21
30 miRNAs, and 56 mRNAs was established, and analysis of this network led to the construction of a sub-
31 network associated with hub lncRNAs. GO and KEGG pathway analyses indicated that the HAE-specific
32 ceRNA network is related to molecular functions and pathways associated with cancer. Subsequent
33 experiments using qPCR and dual-luciferase assays validated the interactions between PCBP1-AS1 and
34 miR-20b-5p, as well as between miR-20b-5p and CAPRIN2. Analysis of the target gene in relation to
35 clinical characteristics of HAE patients suggested that the PCBP1-AS1-miR-20b-5p/CAPRIN2 axis may
36 influence the development of HAE.

37 **Conclusion:**

38 In this study, we described the gene regulation within the lncRNA-miRNA-mRNA ceRNA network
39 during the development of Hepatic Alveolar Echinococcosis (HAE), which contributes to a deeper
40 exploration of the molecular mechanisms underlying HAE. Additionally, we discovered that PCBP1-
41 AS1 may regulate the expression of CAPRIN2 by adsorbing miR-20b-5p, affecting the onset and
42 progression of HAE. PCBP1-AS1 could potentially serve as a useful target for the diagnosis and
43 treatment of HAE.

44 **Keywords:** High-throughput sequencing, Hepatic Alveolar Echinococcosis, long non-coding RNA,
45 competitive endogenous RNA network, lnc-PCBP1-AS1-miR20b-5p/CAPRIN2 axis.

46 **Introduction**

47 Hepatic alveolar echinococcosis (HAE) is a zoonotic disease caused by the larval of the multilocular
48 echinococcus, accounting for 5-10% of the total incidence of echinococcosis^[1]. The growth of HAE is
49 slow and the disease often remains asymptomatic for an extended period, approximately 5 to 15 years.
50 Its growth pattern resembles that of a malignant condition, capable of infiltrating or invading surrounding
51 tissues and organs, and it may even metastasize to distant organs^[2]. Despite the advancements made in
52 the diagnosis and treatment of HAE, the therapeutic outcomes and prognosis are still less than
53 satisfactory^[3]. Research conducted through BLAST sequence analysis of the Echinococcus genome has

54 indicated that approximately one-third of the genes may be unique characteristics of the species and form
55 the basis of its biological traits, which are specific to Echinococcosis. These genes could potentially aid
56 in refining diagnostic methods and identifying novel therapeutic targets^[4]. Therefore, this study
57 preliminarily explores the biological mechanisms and pathogenesis of HAE at the genetic level, in an
58 effort to identify new therapeutic targets to improve treatment outcomes and prognosis.

59 In recent years, advances in sequencing technologies have enabled more in-depth genomic research. It is
60 now known that less than 2% of the human genome encodes proteins. Among the various types of non-
61 coding RNAs (ncRNAs), long non-coding RNAs (lncRNAs) have attracted significant attention. These
62 are defined as long chains of non-coding RNA that exceed 200 base pairs in length and do not have the
63 function of encoding proteins^{[5][6]}. However, through their diverse mechanisms, lncRNAs play functional
64 roles in various cell types, and many lncRNAs possess both tumor-suppressive and oncogenic
65 capabilities^{[7][8]}. Additionally, microRNAs (miRNAs) are endogenous RNA molecules approximately 22
66 base pairs in length that can bind to target RNAs, promoting the degradation of mRNA or inhibiting
67 protein translation^{[9][10]}, they play a crucial role in regulating gene expression and are involved in
68 numerous biological processes through their network of regulatory interactions^{[11][12][13]}.

69 In 2011, Salmena and colleagues first proposed the competitive endogenous RNA (ceRNA) hypothesis.
70 This hypothesis suggests that ceRNAs interact with target miRNAs through miRNA response elements
71 (MREs), thereby regulating the transcriptome on a large scale. Simultaneously, this concept of ceRNAs
72 and their networks offers a novel perspective on the intricate interactions of RNA molecules within the
73 cell, enhancing our comprehension of gene regulation and the potential for targeted therapies in the
74 treatment of diseases^[14]. In recent years, a growing body of research has indicated that lncRNAs can act
75 as ceRNAs, regulating the expression of target mRNAs by competitively sharing miRNAs. They play a
76 significant role in various types of tumors, Such as in hepatocellular carcinoma^[15], pancreatic cancer^[16],
77 gastric cancer^[17], and colorectal cancer^[18]. However, to date, there have been no reports on the study of
78 lncRNAs and ceRNA networks in HAE, and the expression profile of lncRNAs and the associated
79 ceRNA regulatory networks in HAE require further clarification. Therefore, it is particularly important
80 to further understand the role of lncRNAs in the development of HAE and to investigate the pathogenic
81 mechanisms involving ceRNA networks in HAE.

82 In this study, we performed high-throughput sequencing on lesion tissues and adjacent tissues from three
83 HAE patients to identify differentially expressed lncRNAs and mRNAs. Through comprehensive

84 analysis, we constructed a ceRNA network based on the interactions between lncRNA-miRNA and
85 miRNA-mRNA, which will help enhance our understanding of the pathogenesis of HAE, identify new
86 therapeutic targets, improve treatment outcomes, and refine prognosis. Furthermore, our analysis of the
87 Lnc-PCBP1-AS1-miR-20b-5p/CAPRN2 axis revealed that overexpressed Lnc-PCBP1-AS1 may play a
88 key role in the development and progression of HAE by adsorbing miR-20b-5p and thereby targeting the
89 expression of CAPRN2.

90 **Methods**

91 **Patients and Samples**

92 This study collected 13 cases of HAE patients who met the surgical resection criteria at Qinghai
93 Provincial People's Hospital from September 2021 to October 2023. The collected tissues included lesion
94 center tissue, tissue <1cm around the lesion, and tissue >1cm around the lesion. The enrolled patients
95 had no previous history of liver surgery and were not complicated with hepatic cystic echinococcosis,
96 other parasitic diseases, liver benign or malignant tumors, liver abscess, liver metastatic cancer, or other
97 space-occupying liver diseases. Both preoperative imaging and postoperative pathology diagnosed
98 hepatic alveolar echinococcosis. After the specimens were removed, the required tissue samples were
99 quickly cut and placed in RNA-free freezing tubes, then promptly stored in liquid nitrogen at -80°C for
100 subsequent RNA extraction. This study was approved by the Ethics Committee of Qinghai Provincial
101 People's Hospital (approval number 2021-32). All participants voluntarily joined the project and signed
102 an informed consent form. [Table 1](#) presents the clinical data of the 13 HAE patients.

103 Table1 Clinicopathological characteristics of 13 HAE patients.

Clinicopathological characteristics	Patients (N = 13)	
	N	%
Age		
≥40	7	53.8
< 40	6	46.2
Gender		
Male	5	38.5
Female	8	61.5
Lesion size		
≥1040000	4	30.8
< 1040000	9	69.2
Live vascular invasion		

Yes	9	69.2
No	4	30.8
Multiple liver lesions		
Yes	6	46.2
No	7	53.8
Distant metastasis		
Yes	2	15.4
No	11	84.6

104 **RNA Extraction and Sequencing**

105 Total RNA extraction was performed using TRIzol reagent (Thermo Scientific, USA). The RNA samples
106 were assessed using 1% agarose gel electrophoresis, NanoPhotometer® spectrophotometer (Implen, CA,
107 USA), Qubit® 3.0 Fluorometer (Implen, CA, USA), and Agilent 2100 RNA Nano 6000 Assay Kit
108 (Implen, CA, USA). Three micrograms of total RNA from both the central lesion tissue and surrounding
109 tissue of HAE patients were used as starting material for library construction. After library construction,
110 initial quantification was done using Qubit 3.0, and the quality of the libraries was evaluated using the
111 Agilent 2100, Bio-RAD CFX 96 real-time PCR instrument, and Bio-RAD KIT iQ SYBR GRN to ensure
112 library quality. Clustering was followed by paired-end sequencing using the Illumina 4000 high-
113 throughput sequencing platform (HiSeq/MiSeq). Uniquely mapped reads were used for gene read count
114 and FPKM (Fragments Per Kilobase of transcript per Million mapped reads) calculation.

115 **Differentially Expressed Analysis**

116 The R software package DESeq2 was utilized to calculate the differential expression of transcripts using
117 a negative binomial distribution test. The cutoff criteria for identifying differentially expressed genes
118 (DEGs) were set at a P-value <0.05 and a Fold Change (FC) $>2/ <0.5$.

119 **Construction of a ceRNA Regulatory Network**

120 The construction of the ceRNA network involved using the miRcode database
121 (<http://www.mircode.org/>) to match differentially expressed lncRNAs (FC >2 or <0.5 , $P <0.05$) with
122 miRNAs. Based on the miRWalk database (<http://mirwalk.umm.uni-heidelberg.de/>), three
123 bioinformatics algorithms—miRTarBase, miRDB, and TargetScan—were employed to predict the target
124 mRNAs of miRNAs (FC >2 or <0.5 , $P <0.05$). The predicted genes were then intersected with the genes
125 obtained from sequencing. Following data integration, we constructed a comprehensive lncRNA-
126 miRNA-mRNA regulatory network, which was visualized using Cytoscape (version v3.10.1).

127 Additionally, sub-networks were reconstructed using the BinGO plugin in Cytoscape^[19].

128 **Functional Enrichment and Protein–Protein Interaction Analysis**

129 To gain a deeper understanding of the mechanisms by which differentially expressed mRNAs
130 (DEmRNAs) contribute to the development of HAE, we utilized the "clusterProfiler" package in R
131 software for functional annotation analysis. We also employed the ggplot2 package in R to create a
132 bubble chart. $P < 0.05$ was considered a threshold for significance. The protein-protein interaction (PPI)
133 network was established using the STRING online search tool with a combined score of ≥ 0.4 . The PPI
134 network was visualized using Cytoscape (version v3.10.1).

135 **Real-Time Fluorescent Quantitative PCR (qRT-PCR)**

136 We determined the relative expression levels of selected lncRNAs, miRNAs, and mRNAs using qRT-
137 PCR. This study used GAPDH and U6 as internal references for qRT-PCR, and the $2^{-\Delta\Delta C_t}$ method was
138 employed to calculate the relative expression levels of the selected genes. The primer sequences for
139 lncRNAs, mRNAs, and miRNAs, as well as the internal references, are listed in [Table 2](#) and [Table 3](#).

140 Table 2 LncRNA and mRNA primer sequences

Gene symbol	Primer	Sequences (5'-3')
PCBP1-AS1	Forward primer	ATTCCTTACTGACCTGCAT
PCBP1-AS1	Reverse primer	ACTACTCAGTCAATTGCTCCA
CAPRN2	Forward primer	GTGGTGACTCTGGACAAGGA
CAPRN2	Reverse primer	CTAAAGTTCCAGGGGCCAGA
has-GAPDH	Forward primer	TGTTGCCATCAATGACCCCTT
has-GAPDH	Reverse primer	CTCCACGACGTACTIONCAGCG

141 Table 3 miRNA primer sequences

Gene symbol	Primer	Sequences (5'-3')
miR-20b-5p	Forward primer	GCAAAGTGCTCATAGTGCAG
miR-20b-5p	Reverse primer	GGTCCAGTTTTTTTTTTTTTTTCTAC

142 **Cell culture and transfection**

143 The 293T human embryonic kidney cell line was sourced from Promega, and the cells were cultured
144 under conditions of DMEM medium supplemented with 10% FBS and 1% PS, at 37°C in a humidified

145 atmosphere with 5% CO₂. The overexpression plasmids for hsa-miR-20b-5p and the control plasmids
146 were purchased from GeneCopoeia, while the wild-type and mutant plasmids for PCBP1-AS1 and
147 CAPRN2 were obtained from Universal Bio. Transfection of 293T human embryonic kidney cells was
148 carried out using Lipofectamine 3000 reagent (Invitrogen, Shanghai, China), with 0.5µg of plasmid,
149 0.05µM of miRNA, and 1µL of P3000™ reagent. Subsequently, the Dual-Glo® Luciferase assay system
150 was used to measure the luminescence of both firefly and Renilla luciferases. Luciferase activity was
151 represented by the ratio of firefly to Renilla luciferase luminescence intensity. The experiment was
152 conducted independently in triplicate.

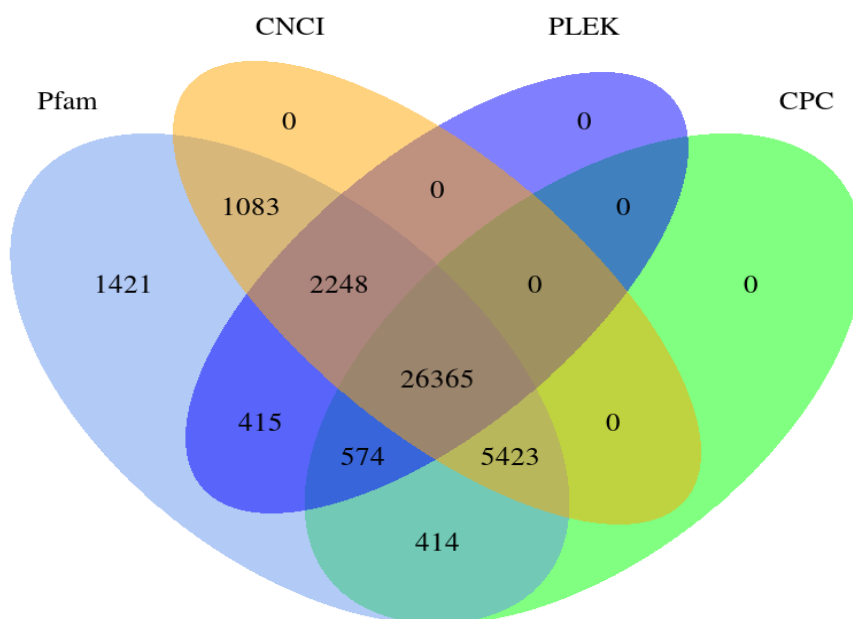
153 **Statistical analysis**

154 Data were statistically analyzed using SPSS 28.0 software (IBM, Armonk, NY, USA) or GraphPad Prism
155 9.0 (GraphPad Software, San Diego, CA, USA). Non-parametric data by group were analyzed using the
156 Friedman rank-sum test, and experimental data are presented in the form of $M (P_{25}, P_{75})$. Student's t-test
157 or one-way analysis of variance (ANOVA) was used to analyze differences between two experimental
158 groups or among more than two groups, respectively. Data were expressed as the mean ± standard
159 deviation (SD). $P < 0.05$ was considered statistically significant.

160 **Results**

161 **Screening for the Coding Potential of LncRNAs**

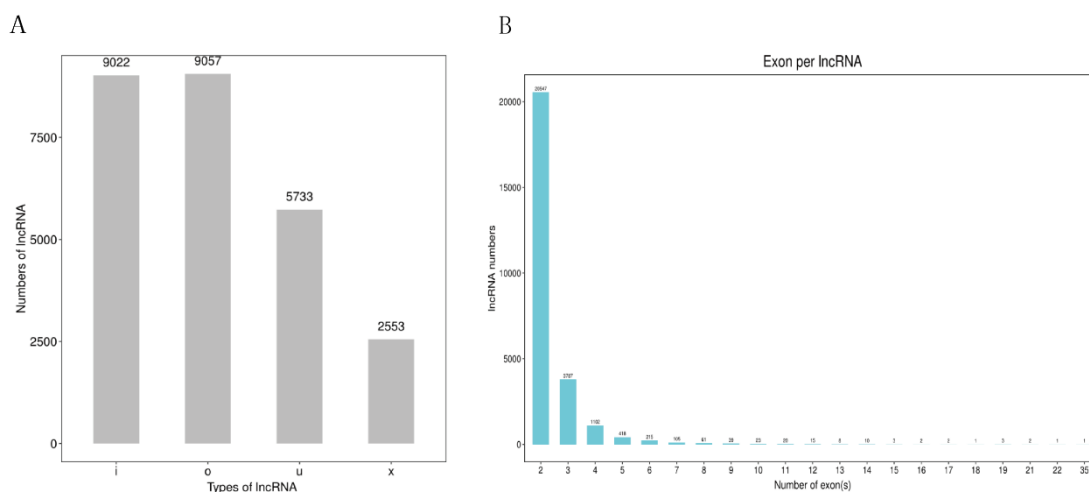
162 We sequenced lncRNAs from the central lesion tissue and surrounding tissue of three patients with
163 human HAE. Since lncRNAs are RNAs that do not encode proteins, we predicted their coding potential
164 to differentiate RNAs with encoding functions from those without encoding potential in the sequencing
165 data. To distinguish lncRNAs, we utilized a comprehensive set of the most widely applied coding
166 potential analysis methods, including: CPC analysis^[20], CNCI analysis^[21], pfam protein domain analysis
167^[22], and PLEK analysis^[23]. Specifically, CPC analysis identified 9,046 lncRNAs, CNCI analysis
168 identified 35,119 lncRNAs, pfam protein domain analysis identified 37,943 lncRNAs, and PLEK
169 analysis identified 2,602 lncRNAs. By integrating the predictions from these four methods, we obtained
170 a total of 26,365 lncRNAs. ([Figure 1](#))



171 Figure 1: Venn diagram showing the results of four coding potential prediction methods.

172 **LncRNA expression profiles in HAE**

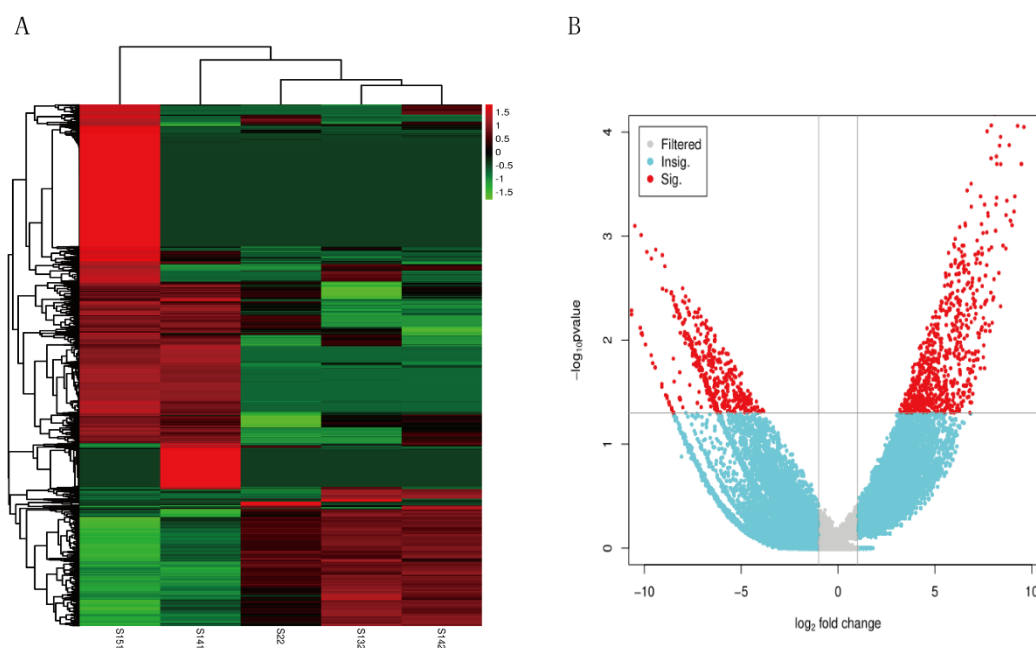
173 To date, tens of thousands of lncRNA genes have been identified in humans and single-celled eukaryotic
 174 organisms. Based on the relative positional relationship between lncRNAs and protein-coding genes,
 175 lncRNAs are classified into intergenic lncRNA (lincRNA), intronic lncRNA, antisense lncRNA, sense
 176 lncRNA, and bidirectional lncRNA^[24]. According to the lncRNA sequencing results, there are 9,022
 177 intronic lncRNAs (denoted as 'i'), 9,057 sense overlapping lncRNAs (denoted as 'o'), 5,733 intergenic
 178 lncRNAs (denoted as 'u'), and 2,553 antisense lncRNAs (denoted as 'x'), with the majority containing
 179 two or more exons (Figure 2).



180 Figure 2: Characteristics of LncRNAs in HAE sequencing. (A) Distribution bar chart of lncRNA types. (B) Bar
 181 chart of the number of exons contained in lncRNA.

182 **The selection of DELncRNAs in HAE**

183 To investigate the expression of LncRNAs in patients with HAE, high-throughput sequencing technology
 184 was employed, with a P-value <0.05 and a fold change (FC) >2 or FC <0.5 as the criteria for screening
 185 differentially expressed LncRNAs (DELncRNAs). A total of 979 DELncRNAs were identified (591
 186 upregulated and 388 downregulated). These differentially expressed LncRNAs are displayed as a
 187 heatmap (Figure 3A) and a volcano plot (Figure 3B), they exhibit good discrimination and clustering
 188 between the central lesion tissue group and the surrounding lesion tissue group. The top 10 up-regulated
 189 and down-regulated DELncRNAs with their names, FoldChange, Log₂FoldChange and P-Value are
 190 listed in Table 4. All DELncRNAs with their names, Fold Change, Log₂FoldChange and P-Value are
 191 listed in Supplementary Table 1.



192 Figure 3: Identification of DELncRNAs in HAE sequencing from lesion tissue and surrounding tissue.
 193 (A) Heatmap of DELncRNAs. (B) Volcano plot of DELncRNAs. Red represents upregulated genes, blue represents
 194 downregulated genes, and gray represents genes without significant differences.

195 Table 4 Top 10 up-regulated and down-regulated lncRNAs

Top 10 up-regulated LncRNAs			
LncRNA	FoldChange	Log ₂ FoldChange	P-Value
ANKRD55	6594.500459	12.68704766	7.57E-07

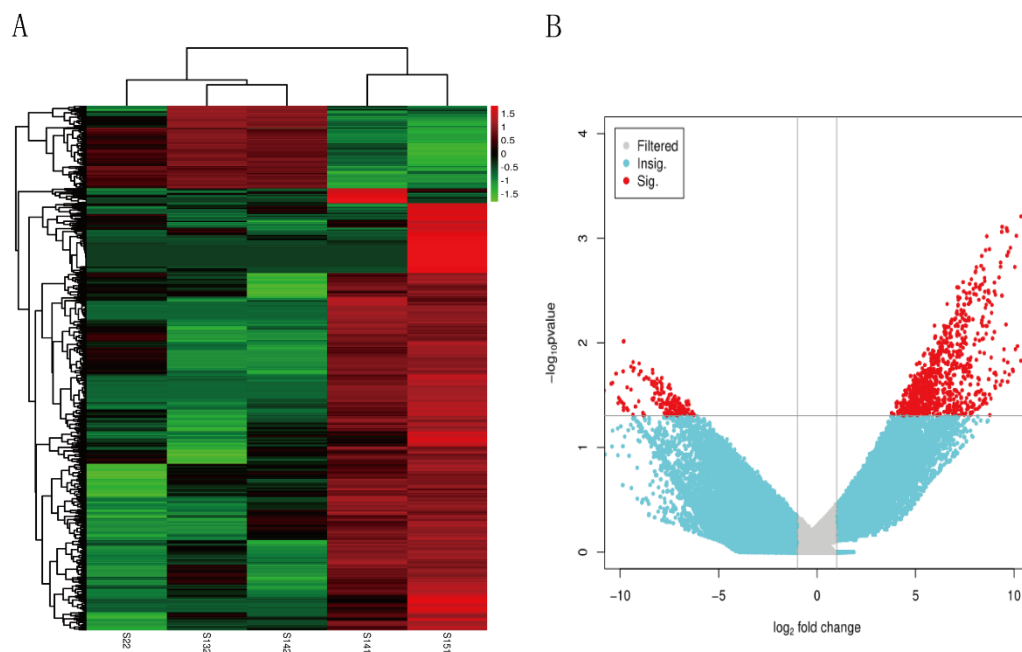
CLK1	1884.50725	10.87997163	3.65E-06
NORAD	793.7336708	9.632511197	9.98E-06
ICAM2	965.9864436	9.915859133	1.33E-05
TCONS_00318939	1187.564098	10.21378967	1.36E-05
IGFBP7	710.1803332	9.472041599	1.43E-05
TCONS_00007400	366.7708817	8.518735296	2.74E-05
ZC3H11A	681.4351841	9.412432629	2.95E-05
H6PD	849.4247064	9.730342261	3.27E-05
FGD5-AS1	413.3040082	8.691059545	4.07E-05

Top 10 down-regulated lncRNAs

lncRNA	FoldChange	Log ₂ FoldChange	P-Value
TCONS_00072674	0.000692128	-10.49667275	0.000800034
NEMF	0.000869933	-10.16680806	0.000977459
TCONS_00156523	0.001466155	-9.413747091	0.00135161
LINC02532	0.001066066	-9.873487282	0.001419007
TCONS_00109132	0.001853407	-9.075604629	0.001522895
TCONS_00222092	0.001251924	-9.641637372	0.001642063
BTD	0.000349111	-11.48402561	0.00185251
TCONS_00268089	0.002029659	-8.944546895	0.001952626
TCONS_00193995	0.003841653	-8.024057163	0.003179705
TCONS_00208765	0.001865792	-9.065995803	0.003205872

196 **DEmRNAs in HAE**

197 Most lncRNAs can act as miRNA sponges, indirectly regulating downstream target genes. To explore
198 the potential "ceRNA" mechanism of lncRNAs in HAE and to reveal the differentially expressed mRNAs
199 in the same tissues, our research group also conducted mRNA sequencing. A total of 870 mRNAs (743
200 upregulated and 127 downregulated) were identified as differentially expressed RNAs (DERNAs) in
201 HAE ($P < 0.05$, $FC > 2 / < 0.5$). These differentially expressed mRNAs are displayed as a heatmap ([Figure](#)
202 [4A](#)) and a volcano plot ([Figure 4B](#)). The top 10 up-regulated and down-regulated DEmRNAs with
203 their names, FoldChange, Log₂FoldChange and P-Value are listed in [Table 5](#). All DEmRNAs with their
204 names, Fold Change, Log₂FoldChange and P-Value are listed in [Supplementary Table 2](#).



205 Figure 4: Identification of DEmRNAs in HAE sequencing from lesion tissue and surrounding tissue. (A) Heatmap
 206 of DEmRNAs. (B) Volcano plot of DEmRNAs. Red represents upregulated genes, blue represents downregulated
 207 genes, and gray represents genes without significant differences.

208 Table5 Top 10 up-regulated and down-regulated mRNAs

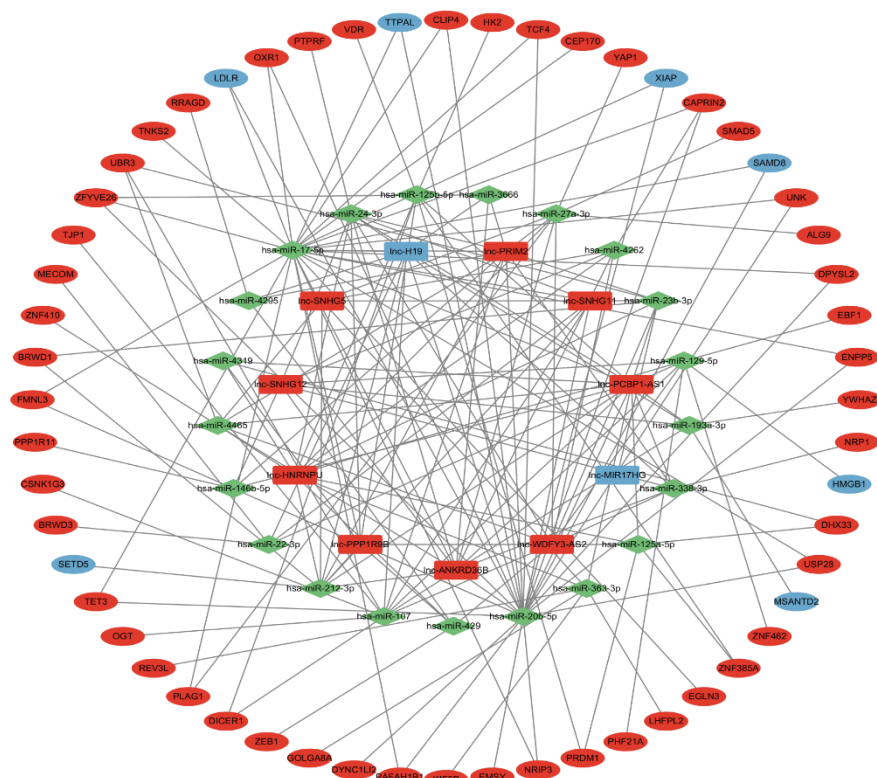
Top 10 up-regulated mRNAs			
mRNA	FoldChange	Log ₂ FoldChange	P-Value
MIER1	6891.139911	12.75052693	5.86E-05
NCK1	4520.924017	12.14240196	0.000119392
METTL9	3199.851264	11.64378913	0.000214831
GTF2H2C	1561.441829	10.60866311	0.000267621
IPMK	1317.737516	10.36384731	0.000618708
FCRL5	673.0462802	9.394561901	0.000778941
SUB1	1486.820226	10.5380145	0.000819456
MORC4	1114.003657	10.12153825	0.000947739
CXorf40B	899.6704652	9.813252852	0.00123812
SPART	429.6831405	8.747129361	0.0012714
Top 10 down-regulated mRNAs			
mRNA	FoldChange	Log ₂ FoldChange	P-Value
CES2	0.001101447	-9.826384333	0.009603027

SURF4	0.001096504	-9.832873188	0.00970853
MDM4	0.00153438	-9.348128419	0.015256378
TPT1	0.001892148	-9.045759259	0.015752727
SYAP1	0.001429811	-9.449960054	0.016911442
SPPL2A	0.001595592	-9.291692341	0.017513725
SLC7A2	0.000359791	-11.44055405	0.017830314
PCYOX1	0.003043029	-8.36027622	0.018166061
LDLR	0.001535247	-9.347313565	0.018465857
WDR36	0.003073114	-8.346082935	0.019419049

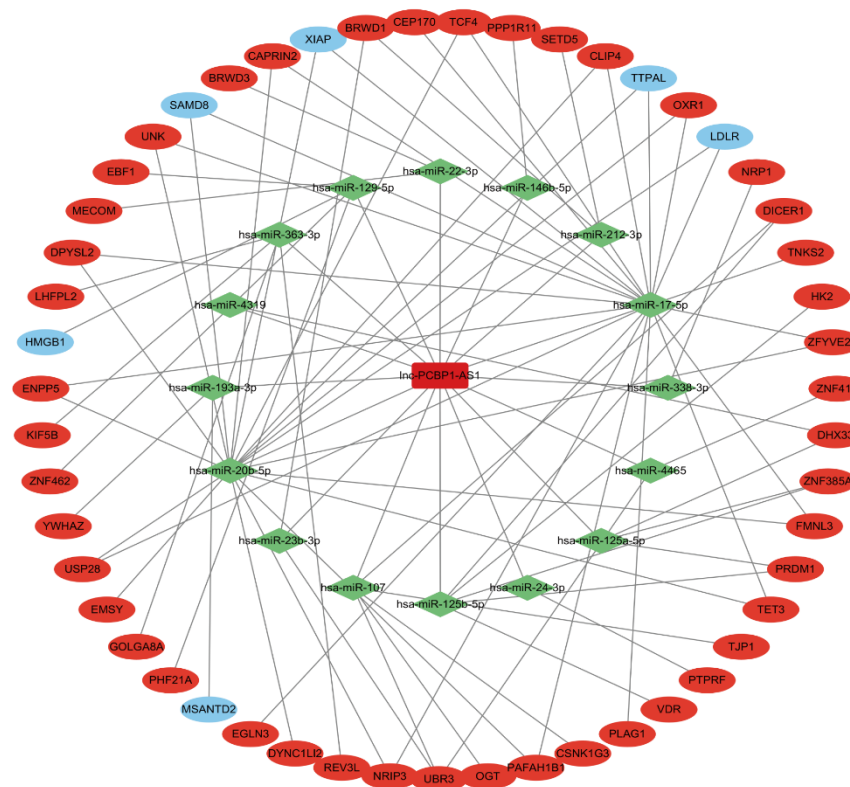
209 **Construction of the ceRNA Network in HAE**

210 As previously mentioned, lncRNAs exert their functions primarily by adsorbing miRNAs. Therefore,
211 based on high-throughput sequencing analysis, we constructed a comprehensive lncRNA-miRNA-
212 mRNA network to study the roles of differentially expressed lncRNAs and mRNAs in HAE. Through
213 the interactions of lncRNA-miRNA and miRNA-mRNA, we obtained a total of 11 lncRNAs, 21 miRNAs,
214 and 56 mRNAs. The constructed lncRNA-miRNA-mRNA ceRNA regulatory network includes 88 nodes
215 and 183 edges ([Figure 5A](#)). It is well known that lncRNAs and mRNAs have co-expression patterns in
216 the ceRNA network. Thus, we selected a hub lncRNA (degree ≥ 16) and its connected miRNAs and
217 mRNAs to reconstruct a sub-network. As shown in ([Figure 5B](#)), the PCBP1-AS1-miRNA-mRNA sub-
218 network consists of 1 lncRNA node, 16 miRNA nodes, 51 mRNA nodes, and 91 edges. The DElncRNA
219 and its matching miRNA and 21 miRNAs and their matching DEMRNAs can be found in ([Table 6](#) and
220 [Table 7](#)). The degree of the ceRNA network were listed in [Supplementary Table 3](#).

A



B



221 Figure 5: Construction of lncRNA-miRNA-mRNA network in HAE. (A) lncRNA-miRNA-mRNA ceRNA
 222 network in HAE. (B) The lncRNA PCBP1-AS1 sub-network. Red nodes indicate up-regulated RNAs while blue
 223 nodes indicate down-regulated RNAs. lncRNAs are denoted by rectangles, miRNAs by light green diamonds, and
 224 mRNAs by ellipses.

225

Table6 DELncRNAs in the ceRNA network were targeted by miRNAs.

DELncRNA	miRNA
lnc-H19	hsa-miR-107,hsa-miR-193a-3p,hsa-miR-338-3p,hsa-miR-22-3p,hsa-miR-4295,hsa-miR-3666, hsa-miR-17-5p,hsa-miR-20b-5p,hsa-miR-212-3p,hsa-miR-24-3p
lnc-PRIM2	hsa-miR-146b-5p, hsa-miR-27a-3p, hsa-miR-4465, hsa-miR-23b-3p, hsa-miR-107, hsa-miR-338-3p, hsa-miR-4295, hsa-miR-3666, hsa-miR-17-5p, hsa-miR-20b-5p, hsa-miR-212-3p, hsa-miR-24-3p
lnc-SNHG11	hsa-miR-22-3p, hsa-miR-107, hsa-miR-17-5p, hsa-miR-20b-5p, hsa-miR-212-3p, hsa-miR-24-3p
lnc-PCBP1-AS1	hsa-miR-363-3p, hsa-miR-129-5p, hsa-miR-125a-5p, hsa-miR-146b-5p, hsa-miR-193a-3p, hsa-miR-4465, hsa-miR-4319, hsa-miR-125b-5p, hsa-miR-23b-3p, hsa-miR-338-3p, hsa-miR-22-3p, hsa-miR-107, hsa-miR-17-5p, hsa-miR-20b-5p, hsa-miR-212-3p, hsa-miR-24-3p
lnc-WDFY3-AS2	hsa-miR-4262, hsa-miR-27a-3p, hsa-miR-129-5p, hsa-miR-429, hsa-miR-4465, hsa-miR-23b-3p, hsa-miR-338-3p, hsa-miR-107, hsa-miR-24-3p
lnc-ANKRD36B	hsa-miR-193a-3p,hsa-miR-4295,hsa-miR-3666,hsa-miR-4262,hsa-miR-27a-3p,hsa-miR-129-5p,hsa-miR-338-3p,hsa-miR-4465,hsa-miR-107,hsa-miR-17-5p,hsa-miR-20b-5p,hsa-miR-212-3p, hsa-miR-24-3p
lnc-PPP1R9B	hsa-miR-125a-5p, hsa-miR-17-5p, hsa-miR-20b-5p, hsa-miR-212-3p, hsa-miR-24-3p, hsa-miR-4319, hsa-miR-125b-5p, hsa-miR-429
lnc-SNHG12	hsa-miR-146b-5p, hsa-miR-193a-3p, hsa-miR-429, hsa-miR-4262, hsa-miR-129-5p, hsa-miR-338-3p, hsa-miR-24-3p
lnc-SNHG5	hsa-miR-363-3p, hsa-miR-27a-3p, hsa-miR-23b-3p, hsa-miR-4262, hsa-miR-4465, hsa-miR-212-3p
lnc-MIR17HG	hsa-miR-23b-3p
lnc-HNRNPU	hsa-miR-363-3p, hsa-miR-4262, hsa-miR-125a-5p, hsa-miR-27a-3p, hsa-miR-4319, hsa-miR-125b-5p, hsa-miR-129-5p, hsa-miR-429, hsa-miR-4465, hsa-miR-23b-3p, hsa-miR-212-3p, hsa-miR-24-3p

226

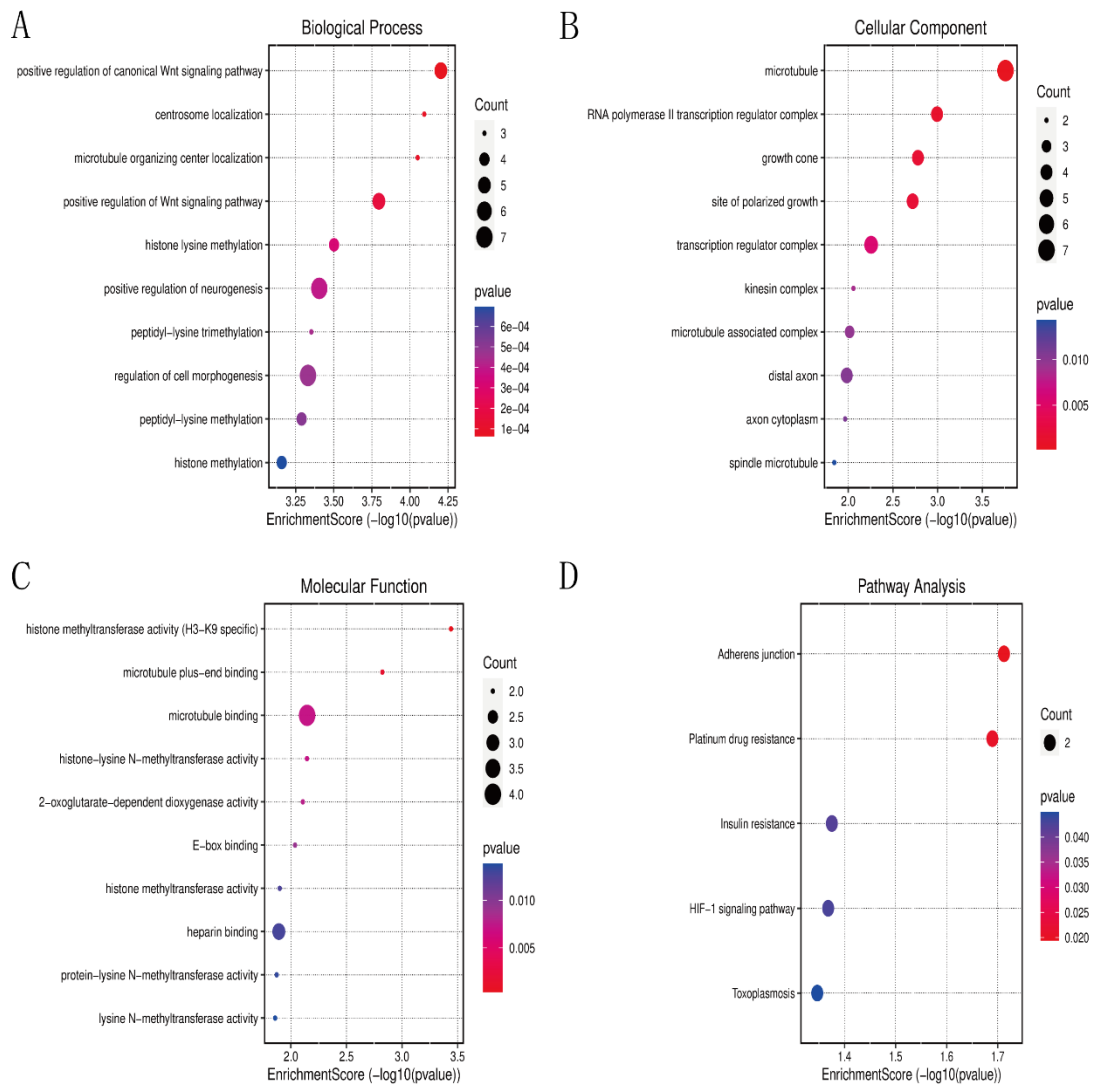
Table7 The 21 miRNAs with their target DEmRNAs in the ceRNA network.

miRNA	DEmRNA
hsa-miR-107	DICER1, OGT, CSNK1G3, TJP1, UBR3
hsa-miR-125a-5p	DHX33, ZNF385A, PRDM1
hsa-miR-146b-5p	PPP1R11
hsa-miR-17-5p	USP28, TCF4, TET3, PAFAH1B1, FMNL3, XIAP, DPYSL2, ZFYVE26, LDLR, TTPAL, ENPP5, NRIP3, EGLN3
hsa-miR-193a-3p	YWHAZ, MSANTD2
hsa-miR-20b-5p	CAPRIN2, EMSY, SP28, TCF4, TET3, PAFAH1B1, FMNL3, DPYSL2, LDLR, TTPAL, ENPP5, NRIP3, SAMD8

hsa-miR-212-3p	SETD5, BRWD1
hsa-miR-24-3p	PTPRF
hsa-miR-27a-3p	YAP1, SMAD5, ALG9, PLAG1
hsa-miR-338-3p	NRP1
hsa-miR-363-3p	LHFPL2, KIF5B, GOLGA8A, REV3L
hsa-miR-4465	UBR3, ZNF410
hsa-miR-4319	DHX33
hsa-miR-125b-5p	ZNF385A, VDR, HK2, DICER1, PRDM1
hsa-miR-23b-3p	BRWD1, UBR3
hsa-miR-129-5p	EBF1, ZNF462, PHF21A, HMGB1
hsa-miR-429	ZEB1
hsa-miR-22-3p	MECOM, BRWD3
hsa-miR-4295	RRAGD
hsa-miR-3666	ZFYVE26
hsa-miR-4262	CAPRIN2

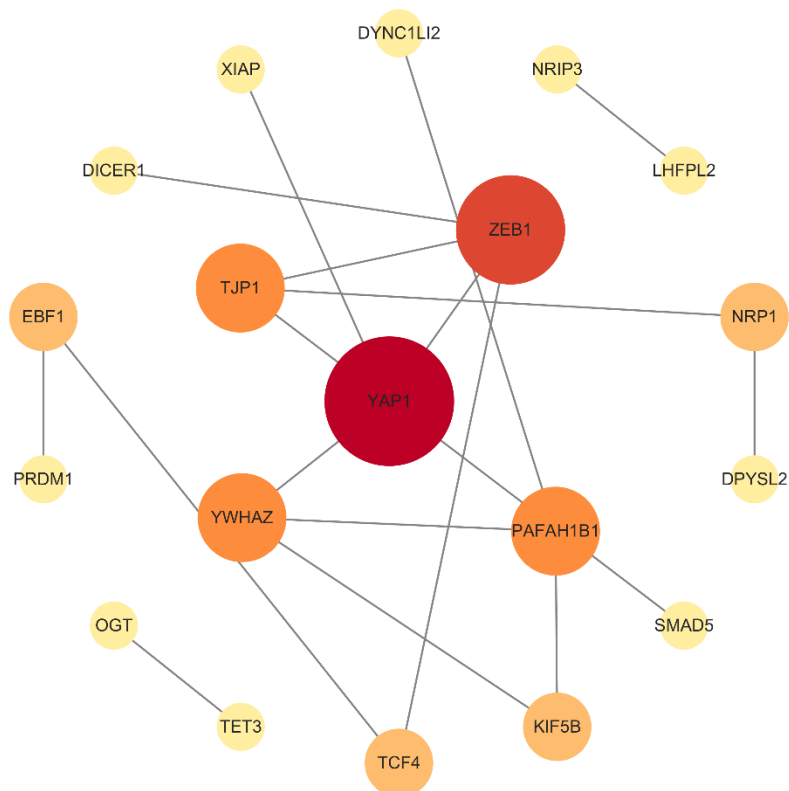
227 **Functional Enrichment Analysis and PPI Network Construction**

228 GO and KEGG enrichment analyses indicate that the DEmRNAs in the ceRNA network are significantly
229 associated with the positive regulation of canonical Wnt signaling pathway, histone lysine methylation,
230 and the positive regulation of the Wnt signaling pathway, among other biological processes (BP) ([Figure](#)
231 [6A](#)). The most enriched Cellular Component (CC) was the cellular microtubule ([Figure 6B](#)). The
232 enrichment of Molecular Functions (MF) was primarily related to histone methyltransferase activity (H3-
233 K9 specific), histone-lysine N-methyltransferase activity and microtubule binding ([Figure](#)
234 [6C](#)). DEmRNAs related to the ceRNA network were significantly enriched in 5 KEGG pathways,
235 namely adherens junction, platinum drug resistance, insulin resistance, HIF-1 signaling pathway, and
236 toxoplasmosis ([Figure 6D](#)). The top 10 results of the functional enrichment analysis are listed in the
237 [Supplementary Table 4](#). The enrichment analysis suggests that the HAE-specific ceRNA network
238 may participate in the pathogenesis and development of HAE by regulating these biological processes
239 and pathways.



240 Figure 6: GO and KEGG enrichment analysis of DEMRNAs in the ceRNA network. (Top10). (A) Bubble Plot of
 241 BP. (B) Bubble Plot of CC. (C) Bubble Plot of MF. (D) Bubble Plot of KEGG.

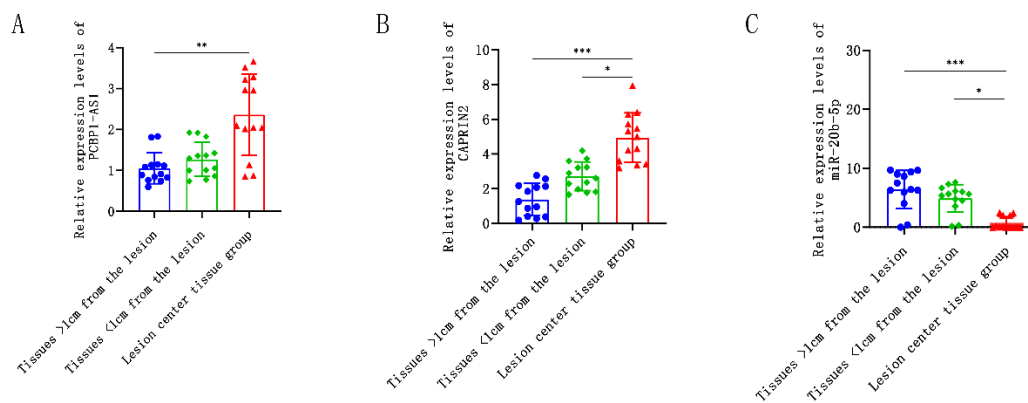
242 Additionally, further analysis was conducted on the interacting mRNAs within the ceRNA network,
243 leading to the construction of a Protein-Protein Interaction (PPI) network. The PPI network comprises
244 19 nodes and 17 edges ([Figure 7](#)). These mRNAs are likely to play a significant role in the disease
245 occurrence and progression of HAE and serve as subjects for subsequent research. Notably, genes with
246 high network degree and comprehensive scores within the network, such as YAP1, ZEB1, PAFAH1B1,
247 TJP1 and YWHA, were found to be primarily enriched in biological processes like "Regulation of
248 developmental process" and "Positive regulation of developmental process". This suggests that these
249 genes are crucial for the development and progression of HAE.



250 Figure 7: The PPI network of DE mRNAs within the ceRNA network. Circles represent DE mRNAs, lines represent
251 interactions between encoded proteins, gradient from dark red to light yellow based on degree.

252 Validation of screened lncRNA-PCBP1-AS1, miR-20b-5p and CAPRIN2 by qRT-PCR.

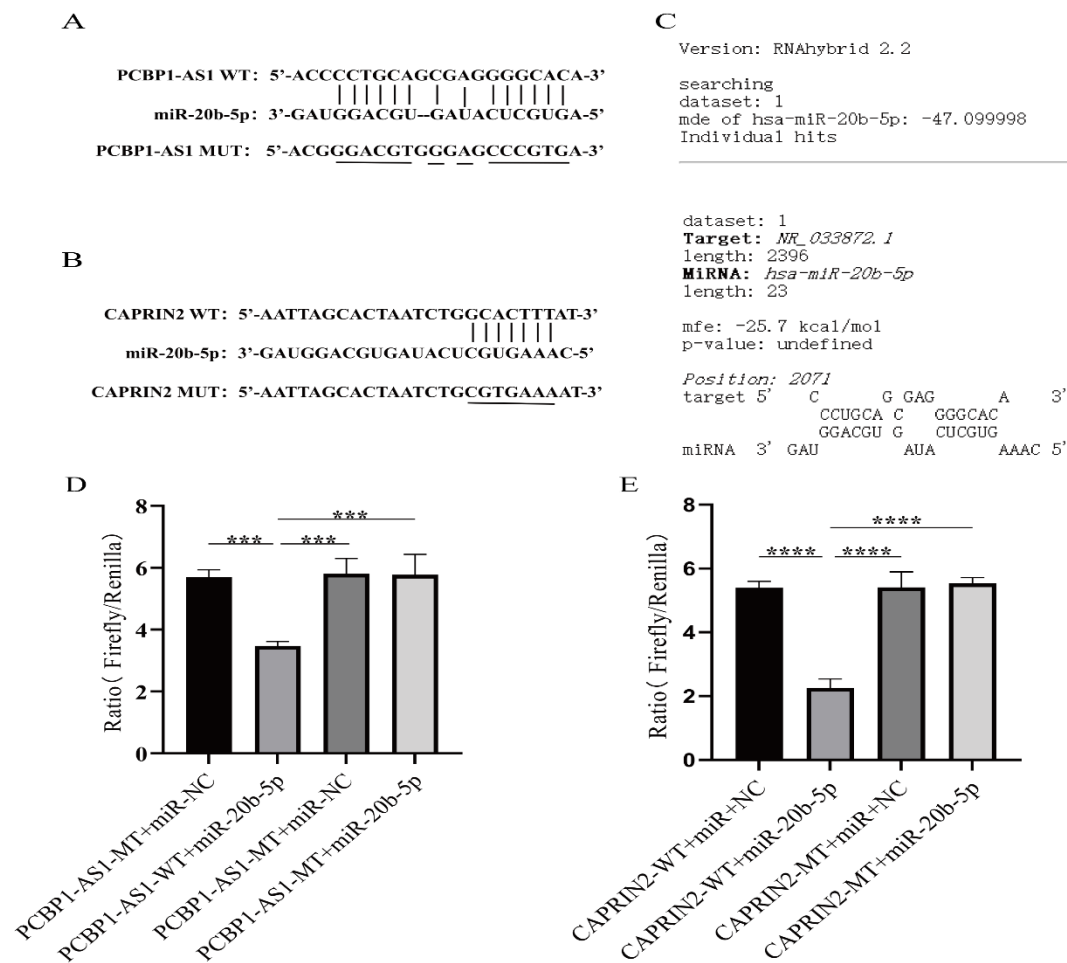
253 We utilized qRT-PCR to analyze the expression levels of PCBP1-AS1, miR-20b-5p, and CAPRIN2 in
254 13 HAE lesion tissues, as well as in tissues less than 1cm and more than 1cm surrounding the lesion. The
255 qRT-PCR results indicated that PCBP1-AS1 and CAPRIN2 were highly expressed ($P < 0.05$) in the lesion
256 tissues ([Figure 8A](#) and [Figure 8B](#)), which is consistent with the results from high-throughput
257 sequencing; whereas miR-20b-5p exhibited low expression ($P < 0.05$) in the HAE lesion tissues ([Figure](#)
258 [8C](#)).



259 Figure 8: Expression of Candidate gene in HAE tissues assessed by qRT-PCR.(A) PCBP1-AS1 expression in
 260 HAE;(B) CAPRN2 expression in HAE;(C) miR-20b-5p expression in HAE. The data are shown as the Median
 261 and interquartile range (IQR). n=13. * $P < 0.05$, ** $P < 0.01$, *** $P < 0.001$.

262 **miR-20b-5p is directly regulated by PCBP1-AS1 and interacts with CAPRN2**

263 In the ceRNA network, there is a targeted binding relationship among PCBP1-AS1, miR-20b-5p, and
 264 CAPRN2. The sequencing data show a consistent expression trend for PCBP1-AS1 and CAPRN2, and
 265 qRT-PCR indicates that both PCBP1-AS1 and CAPRN2 are overexpressed in the lesion tissues, while
 266 miR-20b-5p is underexpressed in the same tissues. Subsequently, we used the RNAhybrid
 267 (<https://bibiserv.cebitec.uni-bielefeld.de/mahybrid>) and Targetscan
 268 databases(<https://www.targetscan.org/>) to predict potential binding sites between PCBP1-AS1 and miR-
 269 20b-5p, as well as between miR-20b-5p and CAPRN2 ([Figure 9A](#) and [Figure 9B](#)), and calculated
 270 the minimum free energy of these binding sites using RNAhybrid ([Figure 9C](#)). In order to further
 271 confirm the predicted results, we transfected them into 293T cells. The results showed that miR-20b-5p
 272 could decrease the fluorescence values in cells transfected with PCBP1-AS1-WT and CAPRN2-WT. In
 273 contrast, there was no significant change in fluorescence values in cells transfected with PCBP1-AS1-
 274 MUT and CAPRN2-MUT ([Figure 9D](#) and [Figure 9E](#)). These results suggest that PCBP1-AS1
 275 directly targets miR-20b-5p, and miR-20b-5p interacts with CAPRN2, with miR-20b-5p expression
 276 being negatively correlated with that of PCBP1-AS1 and CAPRN2.

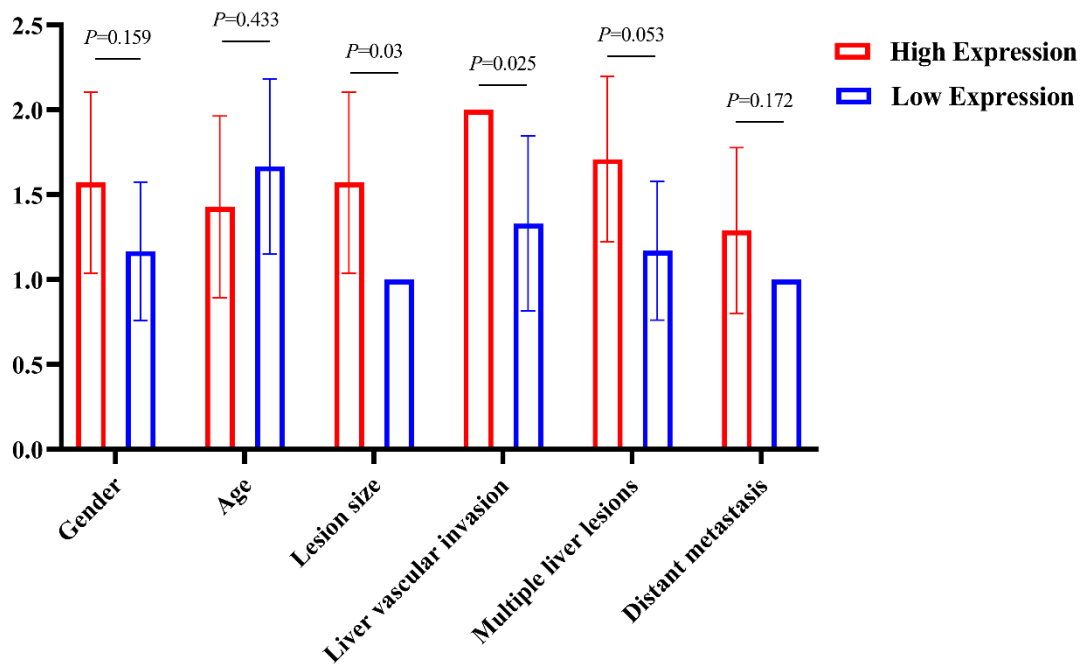


277 Figure 9: (A) The binding sites between miR-20b-5p and PCBP1-AS1;(B) The binding sites between miR-20b-5p
 278 and CAPRIN2;(C) The interaction between THAP9-AS1 and miR-484 and the minimum free energy (mfe) was
 279 predicted with RNAhybrid software;(D) Results of the dual-luciferase assay for miR-20b-5p and PCBP1-AS1;(E)
 280 Results of the dual-luciferase assay for miR-20b-5p and CAPRIN2. The data are shown as the Mean \pm standard
 281 deviation. (n=3). *** $P < 0.001$, **** $P < 0.0001$.

282 Analysis of CAPRIN2 expression in HAE lesions and Clinicopathological characteristics.

283 Through qRT-PCR and dual-luciferase reporter assays, the targeted regulatory relationship among
 284 PCBP1-AS1, miR-20b-5p, and CAPRIN2 has been demonstrated. Specifically, PCBP1-AS1 can affect
 285 the expression of the CAPRIN2 gene by adsorbing miR-20b-5p. To further investigate the association
 286 between this regulatory relationship and the clinical characteristics of HAE patients, we compared the
 287 expression levels of CAPRIN2 with various clinical parameters of the patients. The analysis revealed
 288 that overexpression of CAPRIN2 was not significantly correlated with the patient's sex, age, multiple
 289 intrahepatic lesions, or distant metastasis of HAE ($P > 0.05$), but it was significantly correlated with the

290 size of HAE lesions and intrahepatic vascular invasion ($P < 0.05$) (Figure 10), indicating that patients
291 with overexpressed CAPRIN2 may have a faster disease progression rate than those with low CAPRIN2
292 expression. This could imply that the expression level of CAPRIN2 could serve as a potential biomarker
293 for predicting the prognosis of HAE patients.



294 Figure 10 The expression of CAPRIN2 correlated significantly with Clinicopathological characteristics.
295 These findings suggest that the regulatory axis of PCBP1-AS1-miR-20b-5p/CAPRIN2 may play a key
296 role in controlling the progression and vascular invasion of HAE, which is of great significance for
297 understanding the molecular mechanisms of HAE and developing new therapeutic strategies. Future
298 research can further explore the specific mechanisms of action of this molecular axis and assess its
299 feasibility as a potential therapeutic target.

300 Discussion

301 HAE is a zoonotic disease with severe clinical manifestations and poor prognosis. Currently, radical
302 surgery combined with albendazole medication remains the most ideal treatment option for HAE
303 patients^{[25][26]}. In recent years, numerous studies have gradually revealed the ability of lncRNAs to
304 regulate the expression of target genes through various pathways, playing a significant role in promoting
305 the occurrence, development, and metastasis of tumors. Moreover, the ceRNA hypothesis has proposed
306 an innovative regulatory mechanism, where lncRNAs act as ceRNAs and form extensive regulatory
307 networks by competitively binding to endogenous miRNAs. The imbalance of such ceRNA regulatory

308 networks can significantly affect the biological functions of an organism, leading to the onset of diseases.
309 Additionally, multiple studies have confirmed that ceRNA network play a crucial role in the development
310 of various tumors. However, in HAE, the ceRNA network mediated by lncRNAs has not yet been
311 comprehensively studied, and many ceRNA molecules still await discovery and understanding.
312 In this study, we utilized high-throughput sequencing technology to precisely identify DElncRNAs and
313 DEmRNAs in HAE lesion tissues and their adjacent tissues. We attempted to screen for ceRNA
314 molecules with specific functions using the hierarchical action model of lncRNA-miRNA-mRNA. By
315 integrating the interactions between miRNAs, DEmRNAs, and DElncRNAs, we constructed an HAE-
316 characteristic ceRNA regulatory network, which includes 89 key nodes and 183 interacting edges.
317 Furthermore, we identified hub lncRNAs and built a sub-network centered around PCBP1-AS1.
318 Furthermore, we conducted GO and KEGG enrichment analyses to delve deeper into the biological
319 pathways and functions involved in the ceRNA network for DEmRNAs. The GO enrichment analysis
320 revealed that DEmRNAs in the ceRNA network are primarily involved in the positive regulation of the
321 Wnt signaling pathway and histone lysine methylation, key biological processes that may be significantly
322 associated with the occurrence of HAE. At the molecular level, the DEmRNAs are mainly associated
323 with histone methyltransferase activity (specifically H3-K9) and histone lysine N-methyltransferase
324 activity. Notably, DNA methyltransferase 3A (DNMT3A) is related to histone methyltransferase activity,
325 and DNA methyltransferases are enzymes responsible for methylating DNA in mammals, which can lead
326 to gene silencing^[27]. Moreover, a multitude of histone lysine methyltransferases catalyze various lysine
327 methylation events, decorating the core histones, and their aberrant expression is frequently observed in
328 cancers, developmental disorders, and other pathologies^[28]. In simple terms, HAE may be related to
329 abnormalities in the intracellular epigenetic regulatory mechanisms, which affect gene expression and
330 cellular function.
331 The KEGG pathway enrichment analysis results further revealed the roles of DEmRNAs involved in the
332 ceRNA network across multiple biological pathways, such as adherens junction, platinum drug resistance,
333 insulin resistance, HIF-1 signaling pathway, and toxoplasmosis. The enrichment of these pathways
334 suggests that the pathogenesis of HAE may involve several complex biological processes. It is
335 particularly noteworthy that adherens junctions play a critical role in maintaining the integrity of
336 migrating cell groups, facilitating cell coordination, and cell rearrangement^[29]. They are also implicated
337 in the collective invasion of cancer cells^[30], and adherens junctions mediate adhesive forces between

338 adjacent cells^[31], initiating key intracellular signals that regulate major cellular functions, including
339 proliferation, differentiation, and migration^[32]. Interestingly, the pathogenesis of HAE may be related to
340 the disruption of Kupffer cells^[33] and metabolic pathways^[34], indicating a significant association between
341 adherens junctions and HAE.

342 To systematically analyze the relationships and functions of DEmRNAs involved in the ceRNA network
343 in HAE, we constructed a PPI network. Through this analysis, we identified several genes with high
344 comprehensive scores, such as YAP1, ZEB1, PAFAH1B1, TJP1 and YWHAZ, which are primarily
345 enriched in biological processes related to the regulation of developmental processes. Simultaneously,
346 we observed that YAP1 and YWHAZ have a higher number of nodes in the PPI network, which typically
347 indicates that DEmRNAs with more nodes play a more central role within the network. Research has
348 indicated that YAP1 is one of the most critical effectors of the Hippo pathway and interacts with other
349 pro-oncogenic pathways, promoting cancer development in various ways, including the promotion of
350 malignant phenotypes, expansion of cancer stem cells, and enhancement of cancer cell drug
351 resistance^{[35][36]}. Additionally, YWHAZ has been closely associated with the progression of and as a
352 therapeutic target for various types of cancer, including hepatocellular carcinoma^[37], gastric cancer^[38],
353 and pancreatic cancer^[39]. All in all, these genes are highly relevant to the occurrence and progression of
354 related cancers and merit further research to clarify their roles in HAE.

355 Compelling evidence has shown that lncRNAs can compete for binding sites on miRNAs, thereby
356 regulating the expression of target mRNAs. Within the ceRNA network, we discovered that Lnc-PCBP1-
357 AS1 plays a pivotal role, which may influence variable targets through 16 lncRNA-associated miRNAs.
358 Interestingly, a number of miRNAs, including miR-363^[40], miR-125a-5p^[41], miR-193a^[42], miR-4465^[43],
359 miR-4319^[44], miR-125b-5p^[45], miR-22-3p^[46], miR-107^[47], miR-17-5p^[48], miR-20b-5p^[49], and miR-24-
360 3p^[50], have all been associated with the initiation and progression of hepatocellular carcinoma.
361 Furthermore, miR-20b-5p can be sponged by the lncRNA WWOX-AS1, which upregulates WWOX
362 and thereby inhibits the progression of hepatocellular carcinoma^[51]. The lncRNA MALAT1 can also
363 function as a ceRNA, regulating TXNIP by sequestering miR-20b-5p^[52]. Consequently, the predicted
364 miRNAs can be utilized to identify lncRNAs that play a significant role in gene regulation in HAE,
365 thereby enhancing our comprehension of the ceRNA network.

366 Within the ceRNA network, PCBP1, miR-20b-5p, and CAPRN2 exhibit a high degree of intramodular
367 connectivity, suggesting that they may play a pivotal role in regulating gene expression and biological

368 functions. So, they have been selected as candidate genes for further research. It has been reported that
369 PCBP1-AS1 is closely associated with the proliferation and metastasis of hepatocellular carcinoma^[53].
370 Additionally, the dysregulation of miR-20b-5p has been confirmed in hepatocellular carcinoma, where
371 it negatively regulates CPEB3, affecting the progression of the disease^[54]. Concurrently, our research has
372 discovered that PCBP1-AS1 shares miR-20b-5p response elements with CAPRN2 and regulates the
373 expression of CAPRN2 by spongeing miR-20b-5p. Also, Experiments have validated that CAPRN2 is
374 indeed a genuine target of miR-20b-5p. Besides, the target gene CAPRN2 plays a crucial role in the Wnt
375 signaling pathway^[55], abnormal Wnt signaling is the basis for a variety of human diseases^[56], and
376 dysregulation of the Wnt signaling pathway has been proven to be associated with a range of cancers^[57].
377 Moreover, numerous preclinical experiments have indicated that inhibiting Wnt signaling can prevent
378 the growth and survival of cancer cells^[58]. The aforementioned GO enrichment results indicate that
379 DE mRNAs involved in the ceRNA network in HAE are primarily engaged in the regulation of the Wnt
380 signaling pathway. This suggests that the PCBP1-AS1-miR-20b-5p/CAPRN2 axis may play a key role
381 in HAE through the Wnt signaling pathway. Concurrently, we have analyzed the target gene CAPRN2
382 in relation to clinical characteristics of patients and found that overexpression of CAPRN2 is
383 significantly associated with the size of lesions and the extent of vascular invasion in the liver in HAE.
384 This suggests that PCBP1-AS1 might control CAPRN2 expression in HAE by binding miR-20b-5p,
385 affecting the HAE start and spread. However, the specific mechanisms by which the PCBP1-AS1-miR-
386 20b-5p/CAPRN2 axis modulates the development of HAE require further experimental validation.
387 Considering that PCBP1-AS1 is a hub lncRNA in the ceRNA network, it could potentially serve as a
388 target for HAE diagnosis and treatment. Overall, our research enhances the understanding of the
389 regulatory mechanisms of the PCBP1-AS1-miR-20b-5p/CAPRN2 axis in HAE, which may provide
390 valuable insights to advance HAE research.

391 In conclusion, we have constructed a ceRNA network using lncRNA-miRNA and miRNA-mRNA
392 interactions in HAE, laying the groundwork for further investigation into the regulatory mechanisms of
393 HAE. However, this study still has some limitations, such as a lack of extensive experiments and a small
394 sample size. Subsequently, we will expand our collection of clinical data based on these findings and
395 conduct a more detailed analysis of the pathogenesis of HAE to clarify the roles of these differentially
396 expressed genes within the ceRNA regulatory network. Equally, we will also focus on how the lnc-
397 PCBP1-AS1-miR-20b-5p/CAPRN2 axis regulates the progression of HAE, its functional and

398 mechanistic aspects, which could lay the foundation for the diagnosis and treatment of HAE.

399 **Author contributions**

400 All authors contributed to the article and approved the submitted version.

401 **Funding**

402 This research was supported in part by the Qinghai Provincial Science and Technology Department under
403 the project "Research on differential expression of LncRNA and circRNA and related signaling pathways
404 in hepatic alveolar echinococcosis." (Project No. 2022-ZJ-747) and "KunLun talents High-end
405 Innovation and Entrepreneurship Talent Program" of Qinghai Province (Youth Talent character [2021]
406 No. 13).

407 **Data availability**

408 The experimental data has been deposited in the Gene Expression Omnibus (GEO) database under the
409 accession number GSE261626.

410 **Conflict of interest**

411 The authors declare that the research was conducted in the absence of any commercial or financial
412 relationships that could be construed as a potential conflict of interest.

413

Reference

- 414 [1] McManus DP, Zhang W, Li J, Bartley PB. Echinococcosis. *Lancet*. 2003 Oct 18;362(9392):1295-304.
- 415 [2] Xu X, Qian X, Gao C, Pang Y, Zhou H, Zhu L, Wang Z, Pang M, Wu D, Yu W, Kong F, Shi D, Guo Y, Su
416 X, Hu W, Yan J, Feng X, Fan H. Advances in the pharmacological treatment of hepatic alveolar
417 echinococcosis: From laboratory to clinic. *Front Microbiol*. 2022 Aug 8; 13:953846.
- 418 [3] Nunnari G, Pinzone MR, Gruttadauria S, Celesia BM, Madeddu G, Malaguarnera G, Pavone P, Cappellani A,
419 Cacopardo B. Hepatic echinococcosis: clinical and therapeutic aspects. *World J Gastroenterol*. 2012 Apr
420 7;18(13):1448-58.
- 421 [4] Zheng H, Zhang W, Zhang L, Zhang Z, Li J, Lu G, Zhu Y, Wang Y, Huang Y, Liu J, Kang H, Chen J, Wang
422 L, Chen A, Yu S, Gao Z, Jin L, Gu W, Wang Z, Zhao L, Shi B, Wen H, Lin R, Jones MK, Brejova B, Vinar
423 T, Zhao G, McManus DP, Chen Z, Zhou Y, Wang S. The genome of the hydatid tapeworm *Echinococcus*
424 *granulosus*. *Nat Genet*. 2013 Oct;45(10):1168-75.
- 425 [5] Kopp F, Mendell JT. Functional Classification and Experimental Dissection of Long Noncoding RNAs. *Cell*.
426 2018 Jan 25;172(3):393-407.
- 427 [6] Djebali S, Davis CA, Merkel A, Dobin A, Lassmann T, Mortazavi A, Tanzer A, Lagarde J, Lin W, Schlesinger
428 F, Xue C, Marinov GK, Khatun J, Williams BA, Zaleski C, Rozowsky J, Röder M, Kokocinski F, Abdelhamid
429 RF, Alioto T, Antoshechkin I, Baer MT, Bar NS, Batut P, Bell K, Bell I, Chakraborty S, Chen X, Chrast J,
430 Curado J, Derrien T, Drenkow J, Dumais E, Dumais J, Duttagupta R, Falconnet E, Fastuca M, Fejes-Toth K,
431 Ferreira P, Foissac S, Fullwood MJ, Gao H, Gonzalez D, Gordon A, Gunawardena H, Howald C, Jha S,
432 Johnson R, Kapranov P, King B, Kingswood C, Luo OJ, Park E, Persaud K, Preall JB, Ribeca P, Risk B,
433 Robyr D, Sammeth M, Schaffer L, See LH, Shahab A, Skancke J, Suzuki AM, Takahashi H, Tilgner H, Trout
434 D, Walters N, Wang H, Wrobel J, Yu Y, Ruan X, Hayashizaki Y, Harrow J, Gerstein M, Hubbard T, Reymond
435 A, Antonarakis SE, Hannon G, Giddings MC, Ruan Y, Wold B, Carninci P, Guigó R, Gingeras TR. Landscape
436 of transcription in human cells. *Nature*. 2012 Sep 6;489(7414):101-8.
- 437 [7] Slack FJ, Chinnaiyan AM. The Role of Non-coding RNAs in Oncology. *Cell*. 2019 Nov 14;179(5):1033-1055.
- 438 [8] Herman AB, Tsitsipatis D, Gorospe M. Integrated lncRNA function upon genomic and epigenomic regulation.
439 *Mol Cell*. 2022 Jun 16;82(12):2252-2266.
- 440 [9] Grimson A, Farh KK, Johnston WK, Garrett-Engele P, Lim LP, Bartel DP. MicroRNA targeting specificity
441 in mammals: determinants beyond seed pairing. *Mol Cell*. 2007 Jul 6;27(1):91-105.
- 442 [10] Baek D, Villén J, Shin C, Camargo FD, Gygi SP, Bartel DP. The impact of microRNAs on protein output.
443 *Nature*. 2008 Sep 4;455(7209):64-71.
- 444 [11] Zhang H, Li Y, Lai M. The microRNA network and tumor metastasis. *Oncogene*. 2010 Feb 18;29(7):937-48.
- 445 [12] Thomson DW, Dinger ME. Endogenous microRNA sponges: evidence and controversy. *Nat Rev Genet*. 2016
446 May;17(5):272-83.
- 447 [13] Tay Y, Rinn J, Pandolfi PP. The multilayered complexity of ceRNA crosstalk and competition. *Nature*. 2014
448 Jan 16;505(7483):344-52.
- 449 [14] Salmena L, Poliseno L, Tay Y, Kats L, Pandolfi PP. A ceRNA hypothesis: the Rosetta Stone of a hidden RNA
450 language? *Cell*. 2011 Aug 5;146(3):353-8.
- 451 [15] Rong Z, Wang Z, Wang X, Qin C, Geng W. Molecular interplay between linc01134 and YY1 dictates
452 hepatocellular carcinoma progression. *J Exp Clin Cancer Res*. 2020 Apr 9;39(1):61.
- 453 [16] Li N, Yang G, Luo L, Ling L, Wang X, Shi L, Lan J, Jia X, Zhang Q, Long Z, Liu J, Hu W, He Z, Liu H, Liu
454 W, Zheng G. lncRNA THAP9-AS1 Promotes Pancreatic Ductal Adenocarcinoma Growth and Leads to a Poor
455 Clinical Outcome via Sponging miR-484 and Interacting with YAP. *Clin Cancer Res*. 2020 Apr 1;26(7):1736-
456 1748.

- 457 [17] Yang XZ, Cheng TT, He QJ, Lei ZY, Chi J, Tang Z, Liao QX, Zhang H, Zeng LS, Cui SZ. LINC01133 as
458 ceRNA inhibits gastric cancer progression by sponging miR-106a-3p to regulate APC expression and the
459 Wnt/ β -catenin pathway. *Mol Cancer*. 2018 Aug 22;17(1):126.
- 460 [18] He F, Song Z, Chen H, Chen Z, Yang P, Li W, Yang Z, Zhang T, Wang F, Wei J, Wei F, Wang Q, Cao J.
461 Long noncoding RNA PVT1-214 promotes proliferation and invasion of colorectal cancer by stabilizing Lin28
462 and interacting with miR-128. *Oncogene*. 2019 Jan;38(2):164-179.
- 463 [19] Maere S, Heymans K, Kuiper M. BiNGO: a Cytoscape plugin to assess overrepresentation of gene ontology
464 categories in biological networks. *Bioinformatics*. 2005 Aug 15;21(16):3448-9.
- 465 [20] Kong L, Zhang Y, Ye ZQ, Liu XQ, Zhao SQ, Wei L, Gao G. CPC: assess the protein-coding potential of
466 transcripts using sequence features and support vector machine. *Nucleic Acids Res*. 2007 Jul;35(Web Server
467 issue): W345-9.
- 468 [21] Sun L, Luo H, Bu D, Zhao G, Yu K, Zhang C, Liu Y, Chen R, Zhao Y. Utilizing sequence intrinsic composition
469 to classify protein-coding and long non-coding transcripts. *Nucleic Acids Res*. 2013 Sep;41(17): e166.
- 470 [22] Finn RD, Bateman A, Clements J, Coggill P, Eberhardt RY, Eddy SR, Heger A, Hetherington K, Holm L,
471 Mistry J, Sonnhammer EL, Tate J, Punta M. Pfam: the protein families database. *Nucleic Acids Res*. 2014
472 Jan;42(Database issue): D222-30.
- 473 [23] Li A, Zhang J, Zhou Z. PLEK: a tool for predicting long non-coding RNAs and messenger RNAs based on an
474 improved k-mer scheme. *BMC Bioinformatics*. 2014 Sep 19;15(1):311.
- 475 [24] Ponting CP, Oliver PL, Reik W. Evolution and functions of long noncoding RNAs. *Cell*. 2009 Feb
476 20;136(4):629-41.
- 477 [25] Maimaitiniyati Y, Meng Y, Chen X. Is long-term follow-up without surgical treatment a valid option for
478 hepatic alveolar echinococcosis? *World J Gastroenterol*. 2022 Jun 28;28(24):2775-2777.
- 479 [26] Nunnari G, Pinzone MR, Gruttadauria S, Celesia BM, Madeddu G, Malaguarnera G, Pavone P, Cappellani A,
480 Cacopardo B. Hepatic echinococcosis: clinical and therapeutic aspects. *World J Gastroenterol*. 2012 Apr
481 7;18(13):1448-58.
- 482 [27] Fuks F, Hurd PJ, Deplus R, Kouzarides T. The DNA methyltransferases associate with HP1 and the SUV39H1
483 histone methyltransferase. *Nucleic Acids Res*. 2003 May 1;31(9):2305-12.
- 484 [28] Husmann D, Gozani O. Histone lysine methyltransferases in biology and disease. *Nat Struct Mol Biol*. 2019
485 Oct;26(10):880-889.
- 486 [29] Peglion F, Llense F, Etienne-Manneville S. Adherens junction treadmill during collective migration. *Nat*
487 *Cell Biol*. 2014 Jul;16(7):639-51.
- 488 [30] Friedl P, Gilmour D. Collective cell migration in morphogenesis, regeneration and cancer. *Nat Rev Mol Cell*
489 *Biol*. 2009 Jul;10(7):445-57.
- 490 [31] Smutny M, Yap AS. Neighborly relations: cadherins and mechanotransduction. *J Cell Biol*. 2010 Jun
491 28;189(7):1075-7.
- 492 [32] Harris TJ, Tepass U. Adherens junctions: from molecules to morphogenesis. *Nat Rev Mol Cell Biol*. 2010
493 Jul;11(7):502-14.
- 494 [33] Liu Y, Tian F, Shan J, Gao J, Li B, Lv J, Zhou X, Cai X, Wen H, Ma X. Kupffer Cells: Important Participant
495 of Hepatic Alveolar Echinococcosis. *Front Cell Infect Microbiol*. 2020 Jan 29; 10:8.
- 496 [34] Lin C, Chen Z, Zhang L, Wei Z, Cheng KK, Liu Y, Shen G, Fan H, Dong J. Deciphering the metabolic
497 perturbation in hepatic alveolar echinococcosis: a 1H NMR-based metabolomics study. *Parasit Vectors*. 2019
498 Jun 13;12(1):300.
- 499 [35] Johnson R, Halder G. The two faces of Hippo: targeting the Hippo pathway for regenerative medicine and
500 cancer treatment. *Nat Rev Drug Discov*. 2014 Jan;13(1):63-79.

- 501 [36] Pan D. The hippo signaling pathway in development and cancer. *Dev Cell*. 2010 Oct 19;19(4):491-505.
- 502 [37] Zhao JF, Zhao Q, Hu H, Liao JZ, Lin JS, Xia C, Chang Y, Liu J, Guo AY, He XX. The ASH1-miR-375-
503 YWHAZ Signaling Axis Regulates Tumor Properties in Hepatocellular Carcinoma. *Mol Ther Nucleic Acids*.
504 2018 Jun 1; 11:538-553.
- 505 [38] Liu J, Song S, Lin S, Zhang M, Du Y, Zhang D, Xu W, Wang H. Circ-SERPINE2 promotes the development
506 of gastric carcinoma by sponging miR-375 and modulating YWHAZ. *Cell Prolif*. 2019 Jul;52(4): e12648.
- 507 [39] Cao F, Jiang Y, Chang L, Du H, Chang D, Pan C, Huang X, Yu D, Zhang M, Fan Y, Bian X, Li K. High-
508 throughput functional screen identifies YWHAZ as a key regulator of pancreatic cancer metastasis. *Cell Death*
509 *Dis*. 2023 Jul 14;14(7):431.
- 510 [40] Zhou P, Huang G, Zhao Y, Zhong D, Xu Z, Zeng Y, Zhang Y, Li S, He F. MicroRNA-363-mediated
511 downregulation of S1PR1 suppresses the proliferation of hepatocellular carcinoma cells. *Cell Signal*. 2014
512 Jun;26(6):1347-54.
- 513 [41] Kim JK, Noh JH, Jung KH, Eun JW, Bae HJ, Kim MG, Chang YG, Shen Q, Park WS, Lee JY, Borlak J, Nam
514 SW. Sirtuin7 oncogenic potential in human hepatocellular carcinoma and its regulation by the tumor
515 suppressors MiR-125a-5p and MiR-125b. *Hepatology*. 2013 Mar;57(3):1055-67.
- 516 [42] Salvi A, Conde I, Abeni E, Arici B, Grossi I, Specchia C, Portolani N, Barlati S, De Petro G. Effects of miR-
517 193a and sorafenib on hepatocellular carcinoma cells. *Mol Cancer*. 2013 Dec 13; 12:162.
- 518 [43] Bu WJ, Fang Z, Li WL, Wang X, Dong MJ, Tao QY, Zhang L, Xu YQ. LINC00240 sponges miR-4465 to
519 promote proliferation, migration, and invasion of hepatocellular carcinoma cells via HGF/c-MET signaling
520 pathway. *Eur Rev Med Pharmacol Sci*. 2020 Oct;24(20):10452-10461.
- 521 [44] Han S, Shi Y, Sun L, Liu Z, Song T, Liu Q. MiR-4319 induced an inhibition of epithelial-mesenchymal
522 transition and prevented cancer stemness of HCC through targeting FOXQ1. *Int J Biol Sci*. 2019 Nov
523 15;15(13):2936-2947.
- 524 [45] Lin XH, Li DP, Liu ZY, Zhang S, Tang WQ, Chen RX, Weng SQ, Tseng YJ, Xue RY, Dong L. Six immune-
525 related promising biomarkers may promote hepatocellular carcinoma prognosis: a bioinformatics analysis and
526 experimental validation. *Cancer Cell Int*. 2023 Mar 23;23(1):52.
- 527 [46] Cui S, Chen Y, Guo Y, Wang X, Chen D. Hsa-miR-22-3p inhibits liver cancer cell EMT and cell migration/
528 invasion by indirectly regulating SPRY2. *PLoS One*. 2023 Feb 7;18(2): e0281536.
- 529 [47] Chen HA, Li CC, Lin YJ, Wang TF, Chen MC, Su YH, Yeh YL, Padma VV, Liao PH, Huang CY. Hsa-miR-
530 107 regulates chemosensitivity and inhibits tumor growth in hepatocellular carcinoma cells. *Aging (Albany*
531 *NY)*. 2021 Apr 26;13(8):12046-12057.
- 532 [48] Yang F, Yin Y, Wang F, Wang Y, Zhang L, Tang Y, Sun S. miR-17-5p Promotes migration of human
533 hepatocellular carcinoma cells through the p38 mitogen-activated protein kinase-heat shock protein 27
534 pathway. *Hepatology*. 2010 May;51(5):1614-23.
- 535 [49] Li Z, Wu L, Tan W, Zhang K, Lin Q, Zhu J, Tu C, Lv X, Jiang C. MiR-20b-5p promotes hepatocellular
536 carcinoma cell proliferation, migration and invasion by down-regulating CPEB3. *Ann Hepatol*. 2021 Jul-Aug;
537 23:100345.
- 538 [50] Fan JC, Zeng F, Le YG, Xin L. LncRNA CASC2 inhibited the viability and induced the apoptosis of
539 hepatocellular carcinoma cells through regulating miR-24-3p. *J Cell Biochem*. 2018 Aug;119(8):6391-6397.
- 540 [51] Xu D, Liu X, Wu J, Wang Y, Zhou K, Chen W, Chen J, Chen C, Chen L. LncRNA WWOX-AS1 sponges
541 miR-20b-5p in hepatocellular carcinoma and represses its progression by upregulating WWOX. *Cancer Biol*
542 *Ther*. 2020 Oct 2;21(10):927-936.
- 543 [52] Li JZ, Ye LH, Wang DH, Zhang HC, Li TY, Liu ZQ, Dai EH, Li MR. The identify role and molecular
544 mechanism of the MALAT1/hsa-mir-20b-5p/TXNIP axis in liver inflammation caused by CHB in patients

- 545 with chronic HBV infection complicated with NAFLD. *Virus Res.* 2021 Jun; 298:198405.
- 546 [53] Luo T, Gao Y, Zhangyuan G, Xu X, Xue C, Jin L, Zhang W, Zhu C, Sun B, Qin X. lncRNA PCBP1-AS1
547 Aggravates the Progression of Hepatocellular Carcinoma via Regulating PCBP1/PRL-3/AKT Pathway.
548 *Cancer Manag Res.* 2020 Jul 6; 12:5395-5408.
- 549 [54] Li Z, Wu L, Tan W, Zhang K, Lin Q, Zhu J, Tu C, Lv X, Jiang C. MiR-20b-5p promotes hepatocellular
550 carcinoma cell proliferation, migration and invasion by down-regulating CPEB3. *Ann Hepatol.* 2021 Jul-Aug;
551 23:100345.
- 552 [55] Ding Y, Xi Y, Chen T, Wang JY, Tao DL, Wu ZL, Li YP, Li C, Zeng R, Li L. Caprin-2 enhances canonical
553 Wnt signaling through regulating LRP5/6 phosphorylation. *J Cell Biol.* 2008 Sep 8;182(5):865-72.
- 554 [56] Clevers H, Nusse R. Wnt/ β -catenin signaling and disease. *Cell.* 2012 Jun 8;149(6):1192-205.
- 555 [57] Zhan T, Rindtorff N, Boutros M. Wnt signaling in cancer. *Oncogene.* 2017 Mar;36(11):1461-1473.
- 556 [58] Polakis P. Wnt signaling in cancer. *Cold Spring Harb Perspect Biol.* 2012 May 1;4(5): a008052.